

## Synthesis of CeO<sub>2</sub> Nanorods via Ultrasonication Assisted by Polyethylene Glycol

Dengsong Zhang,<sup>\*,†,‡</sup> Hongxia Fu,<sup>†</sup> Liyi Shi,<sup>\*,†,‡</sup> Chengsi Pan,<sup>†</sup> Qiang Li,<sup>§</sup> Yuliang Chu,<sup>§</sup> and Weijun Yu<sup>§</sup>

Department of Chemistry, Shanghai University, Shanghai, 200444, China, School of Material Science and Engineering, Shanghai University, Shanghai 200072, China, and Center of Analysis and Test, Shanghai University, Shanghai, 200444, China

Received September 8, 2006

Polycrystalline CeO<sub>2</sub> nanorods 5–10 nm in diameter and 50–150 nm in length were synthesized via ultrasonication using polyethylene glycol (PEG) as a structure-directing agent at room temperature. The properties of the CeO<sub>2</sub> nanorods were characterized by TEM, EDS, XRD, XPS, FT-IR, TG, BET, and UV–vis spectroscopy. Various reaction parameters, such as the content of PEG, the molecular weight of PEG, the concentration of KOH, the pH value, and the sonication time, were investigated by a series of control experiments. The content of PEG, the molecular weight of PEG, and the sonication time were confirmed to be the crucial factors determining the formation of one-dimensional CeO<sub>2</sub> nanorods. A possible ultrasonic formation mechanism has been suggested to explain the formation of CeO<sub>2</sub> nanorods.

### Introduction

One-dimensional (1-D) nanomaterials are expected to play a key role in future nanotechnology as well as to provide model systems to demonstrate quantum size effects.<sup>1</sup> One-dimensional nanomaterials offer great potential as building blocks for applications in nanoelectronics, photonics, and other uses.<sup>2</sup> Recently, nanorods have attracted enormous technological and scientific interest. Many metal oxide nanorods, such as SnO<sub>2</sub>,<sup>3</sup> MgO,<sup>4</sup> ZnO,<sup>5</sup> Al<sub>2</sub>O<sub>3</sub>,<sup>6</sup> CuO,<sup>7,8</sup> Mn<sub>2</sub>O<sub>3</sub>,<sup>9</sup> MoO<sub>3</sub>,<sup>10</sup> PbO<sub>2</sub>,<sup>11</sup> Co<sub>3</sub>O<sub>4</sub>,<sup>12</sup> VO<sub>x</sub>,<sup>13</sup> Eu<sub>2</sub>O<sub>3</sub>,<sup>14</sup> and so on, have been synthesized by electrochemistry, template,

emulsion or polymeric system, arc discharge, laser-assisted catalysis, hydrothermal, and ultrasonication methods in the past several years.

Polyethylene glycol (PEG), an inexpensive surfactant, has been used to assist the formation of metal oxide nanorods in the previous research, which needs no complicated procedure, without hard template supporting and relatively low temperature.<sup>15–17</sup> For example, Lian et al.<sup>16</sup> used PEG1000 to synthesize Fe<sub>3</sub>O<sub>4</sub> nanorods by a hydrothermal method at 150 °C. Li et al.<sup>17</sup> reported a selected-control synthesis of ZnO nanowires and nanorods using PEG by a hydrothermal method at 140 °C.

Ultrasonication, a simple and efficient method, has been successfully used to prepare nanorods. Zhang et al.<sup>18</sup> synthesized Ag nanorods and nanofibers in sodium bis(2-

\* To whom correspondence should be addressed. E-mail: dengsongzh@163.com (D.Z.), sly0726@163.com (L.S.). Fax: +86-21-66134852.

<sup>†</sup> Department of Chemistry.

<sup>‡</sup> School of Material Science and Engineering.

<sup>§</sup> Center of Analysis and Test.

- (1) Ma, D. D. D.; Lee, C. S.; Au, F. C. K.; Tong, S. Y.; Lee, S. T. *Science* **2003**, *299*, 1874.
- (2) Huang, Y.; Duan, X.; Wei, Q.; Lieber, C. M. *Science* **2001**, *291*, 630.
- (3) Pan, Z. W.; Dai, Z. R.; Wang, Z. L. *Science* **2001**, *291*, 1947.
- (4) Yang, P. D.; Lieber, C. M. *Science* **1996**, *273*, 1836.
- (5) Huang, M. H.; Mao, S.; Feick, H.; Yan, H. Q.; Qu, Y. Y.; Kind, H.; Weber, E.; Russo, R.; Yang, P. D. *Science* **2001**, *292*, 1897.
- (6) Zhu, H. Y.; Gao, X. P.; Song, D. Y.; Bai, Y. Q.; Ringer, S. P.; Gao, Z.; Xi, Y. X.; Martens, W.; Riches, J. D.; Frost, R. L. *J. Phys. Chem. B* **2004**, *108*, 4245.
- (7) Gao, X. P.; Bao, J. L.; Pan, G. L.; Zhu, H. Y.; Huang, P. X.; Wu, F.; Song, D. Y. *J. Phys. Chem. B* **2004**, *18*, 5547.
- (8) Wang, W.; Zhan, Y.; Wang, G. *Chem. Commun.* **2001**, 727.
- (9) Yuan, Z. Y.; Ren, T. Z.; Du, G.; Su, B. L. *Chem. Phys. Lett.* **2004**, *389*, 83.

- (10) Patzke, G. R.; Michailovski, A.; Krumeich, F.; Nesper, R.; Grunwaldt, J.-D.; Baiker, A. *Chem. Mater.* **2004**, *16*, 1126.
- (11) Cao, M.; Hu, C.; Peng, G.; Qi, Y.; Wang, E. *J. Am. Chem. Soc.* **2003**, *125*, 4982.
- (12) Xu, R.; Zeng, H. C. *J. Phys. Chem. B* **2003**, *107*, 12643.
- (13) Spahr, M. E.; Bitterli, P.; Nesper, R.; Muller, M.; Krumeich, F.; Nissen, H.-U. *Angew. Chem., Int. Ed.* **1998**, *37*, 1263.
- (14) Pol, V. G.; Palchik, O.; Gedanken, A.; Felner, I. *J. Phys. Chem. B* **2002**, *106*, 9737.
- (15) Feldmann, C. *Solid State Sci.* **2005**, *7*, 868.
- (16) Lian, S.; Kang, Z.; Wang, E.; Jiang, M.; Hu, C.; Xu, L. *Solid State Commun.* **2003**, *127*, 605.
- (17) Li, Z.; Xiong, Y.; Xie, Y. *Inorg. Chem.* **2003**, *42*, 8105.
- (18) Zhang, J.; Han, B.; Liu, M.; Liu, D.; Dong, Z.; Liu, J.; Li, D.; Wang, J.; Dong, B.; Zhao, H.; Rong, L. *J. Phys. Chem. B* **2003**, *107*, 3679.

ethylhexyl) sulfosuccinate/isooctane reverse micelles with the aid of ultrasonication. Wang et al.<sup>8</sup> reported an anhydrous solid-state reaction in the presence of PEG to synthesize CuO nanorods via ultrasonication. Pol et al.<sup>14</sup> synthesized Eu<sub>2</sub>O<sub>3</sub> nanorods by thermal conversion (700 °C) of amorphous Eu(OH)<sub>3</sub> nanorods prepared with ultrasonication.

CeO<sub>2</sub> is a technologically important rare earth material because of its wide applications as polishing materials,<sup>19</sup> fuel cells,<sup>20</sup> oxygen sensors,<sup>21</sup> catalysts,<sup>22</sup> and UV blockers.<sup>23</sup> Recently, the synthesis of CeO<sub>2</sub> nanorods/nanowires has been of great interest in fundamental study. Zhou et al.<sup>24</sup> and Huang et al.<sup>25</sup> synthesized CeO<sub>2</sub> nanorods 15–30 nm in diameter by a precipitation method combined with hydrothermal treatment. La et al.<sup>26</sup> and Wu et al.<sup>27</sup> fabricated CeO<sub>2</sub> nanowires 60–70 nm in diameter using anodic alumina membranes as templates. Sun et al.<sup>28</sup> synthesized CeO<sub>2</sub> nanowires 30–120 nm in diameter by a precipitation method combined with thermostatic treatment using sodium bis(2-ethylhexyl) sulfosuccinate as templates. By a similar method, Vantomme et al.<sup>29</sup> and Yang and Guo<sup>30</sup> synthesized CeO<sub>2</sub> nanowires 10–25 nm in diameter using cetyltrimethylammonium bromide (CTMABr) and octadecyl-amine, respectively. In the previous reports, the synthesis methods of CeO<sub>2</sub> nanorods/nanowires are relatively complicated and always need high-temperature, high-pressure, or long-time treatments. The one-step synthesis of CeO<sub>2</sub> nanorods is still a challenge. Moreover, to the best of our knowledge, no reports on the simple synthesis of CeO<sub>2</sub> nanorods of <10 nm diameter have been published to date.

Recently, CeO<sub>2</sub> nanoparticles<sup>31</sup> and nanotubes<sup>32</sup> prepared by ultrasonication have been reported. In addition, Qi et al.<sup>33</sup> synthesized CeO<sub>2</sub> microrods (200–250 nm in diameter and 600–1200 nm in length) by thermal conversion (500 °C) of CeOHCO<sub>3</sub> microrods prepared with ultrasonication. We have synthesized 1-D CeO<sub>2</sub> composite nanowires using carbon

nanotubes as templates via ultrasonication.<sup>34</sup> However, CeO<sub>2</sub> nanorods have never been synthesized via ultrasonication at room temperature.

Herein, we report a simple liquid-phase synthesis method for CeO<sub>2</sub> nanorods of <10 nm diameter using the cheap surfactant, PEG, as a structure-directing agent via ultrasonication at room temperature.

## Experimental Section

**Synthesis.** All chemicals were of analytical grade and were used as purchased without further purification. PEG (*M<sub>w</sub>* 200, 600, 2000, and 20 000), NaOH, Ce(NO<sub>3</sub>)<sub>3</sub>, and commercial CeO<sub>2</sub> powders were all supplied by Shanghai Chemical Reagent Company (P. R. China). Deionized water was used throughout.

In a typical synthesis, 1 g of PEG600 was first dispersed in 100 mL of 0.05 g/mL Ce(NO<sub>3</sub>)<sub>3</sub> solution (the content of PEG600 is 1%) by ultrasonication at room temperature, and then 0.005 g/mL NaOH solution was added gradually (5 mL/min) into the above-mixed solutions with vigorous stirring during the ultrasonication until the pH value was 10. It takes ~1 h for this step. Finally, the colloidal precipitates, which still exist in the solution, were further sonicated for 1 h. It is noted that the sonication was kept at room temperature in air throughout by a cooling system. After rinsing repeatedly with alcohol to remove PEG600 and drying at 100 °C in air for 1 day, the final product was obtained. In this experiment, the overall yield of a single run is ~3 g.

**Characterization.** The nanorods were observed by a field emission transmission electron microscope (FE-TEM, JEOL JEM-2010F) equipped with an energy-dispersive spectral (EDS) analyzer, and powdered samples were dispersed in absolute ethanol by ultrasonication for 10 min in a KQ-250B ultrasonic bath. A JEOL JSM-6700F scanning electron microscope (SEM) was also employed for the observation of some samples. XRD measurements were performed with Rigaku D/MAX-RB X-ray diffractometer by using Cu K $\alpha$  (40 kV, 40 mA) radiation and a secondary beam graphite monochromator. XPS spectra were recorded on a PHI-5000C ESCA system (Perkin-Elmer) with Al K $\alpha$  radiation. FT-IR spectra were recorded on a Thermo Nicolet Avatar 370 spectrometer using KBr pellets. Thermal gravimetric (TG) analysis of the samples was carried out with a Netzsch STA 409 PG/PC analyzer. The UV-vis spectra of the obtained nanorods dispersed in ethanol were recorded on a SHIMADZU UV-2501 spectrometer using a quartz cell (1 cm path length), and pure ethanol was used as a blank. The BET specific surface area of the samples was characterized by nitrogen adsorption at 77 K with Micromeritics ASAP 2010.

## Results and Discussion

**Characteristics of CeO<sub>2</sub> Nanorods.** The morphology of the as-synthesized sample was obtained with high-resolution TEM (HRTEM). Figure 1, parts a and b, shows the TEM images of the CeO<sub>2</sub> nanorods. CeO<sub>2</sub> nanorods are 50–150 nm in length and have uniform diameters in the range of 5–10 nm. The HRTEM image in Figure 1c shows the clear (111) and (220) lattice fringes with the interplanar spacing of 0.31 and 0.19 nm, respectively, which are the same as the literature values,<sup>35</sup> revealing that the CeO<sub>2</sub> nanorods are composed of many tiny interconnected grains at various

- (19) Feng, X. D.; Sayle, D. C.; Wang, Z. L.; Paras, M. S.; Santora, B.; Sutorik, A. C.; Sayle, T. X. T.; Yang, Y.; Ding, Y.; Wang, X.; Her, Y.-S. *Science* **2006**, *312*, 1504.
- (20) Nair, J. P.; Wachtel, E.; Lubomirsky, I.; Fleig, J.; Maier, J. *Adv. Mater.* **2003**, *15*, 2077.
- (21) Jasinski, P.; Suzuki, T.; Anderson, H. U. *Sens. Actuators, B* **2003**, *95*, 73.
- (22) Lundberg, M.; Skaerman, B.; Cesar, F.; Wallenberg, L. R. *Microporous Mesoporous Mater.* **2002**, *54*, 97.
- (23) Zhang, Y.; Si, R.; Liao, C.; Yan, C. *J. Phys. Chem. B* **2003**, *107*, 10159.
- (24) Zhou, K. B.; Wang, X.; Sun, X. M.; Peng, Q.; Li, Y. D. *J. Catal.* **2005**, *229*, 206.
- (25) Huang, P. X.; Wu, F.; Zhu, B. L.; Gao, X. P.; Zhu, H. Y.; Yan, T. Y.; Huang, W. P.; Wu, S. H.; Song, D. Y. *J. Phys. Chem. B* **2005**, *109*, 19169.
- (26) La, R. J.; Hu, Z. A.; Li, H. L.; Shang, X. L.; Yang, Y. Y. *Mater. Sci. Eng., A* **2004**, *368*, 145.
- (27) Wu, G. S.; Xie, T.; Yuan, X. Y.; Cheng, B. C.; Zhang, L. D. *Mater. Res. Bull.* **2004**, *39*, 1023.
- (28) Sun, C. W.; Li, H.; Wang, Z. X.; Chen, L. Q.; Huang, X. J. *Chem. Lett.* **2004**, *33*, 662.
- (29) Vantomme, A.; Yuan, Z. Y.; Du, G. H.; Su, B. L. *Langmuir* **2005**, *21*, 1132.
- (30) Yang, R.; Guo, L. *J. Mater. Sci.* **2005**, *40*, 1305.
- (31) Yin, L.; Wang, Y.; Pang, G.; Kolytyn, Y.; Gedanken, A. *J. Colloid Interface Sci.* **2002**, *246*, 78.
- (32) Miao, J.; Wang, H.; Li, Y.; Zhu, J.; Zhu, J. *J. Cryst. Growth* **2005**, *281*, 525.
- (33) Qi, R.-J.; Zhu, Y.-J.; Cheng, G.-F.; Huang, Y.-H. *Nanotechnology* **2005**, *16*, 2502.

(34) Zhang, D. S.; Shi, L. Y.; Fu, H. X.; Fang, J. H. *Carbon* **2006**, *44*, 2853.

(35) Mai, H.-X.; Sun, L.-D.; Zhang, Y.-W.; Si, R.; Feng, W.; Zhang, H.-P.; Liu, H.-C.; Yan, C.-H. *J. Phys. Chem. B* **2005**, *109*, 24380.

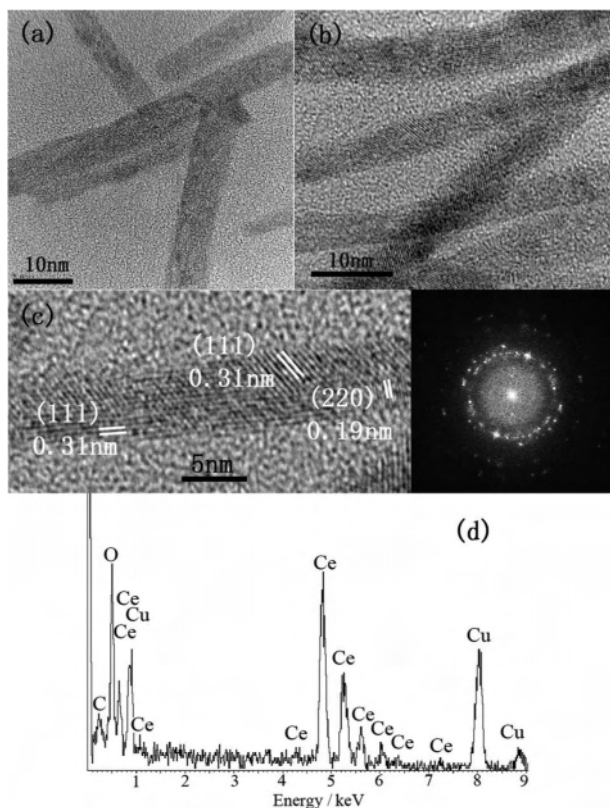


**Figure 1.** (a and b) TEM images of CeO<sub>2</sub> nanorods. (c) HRTEM image of the single nanorod and its ED pattern (inset). (d) EDS spectrum of CeO<sub>2</sub> nanorods.

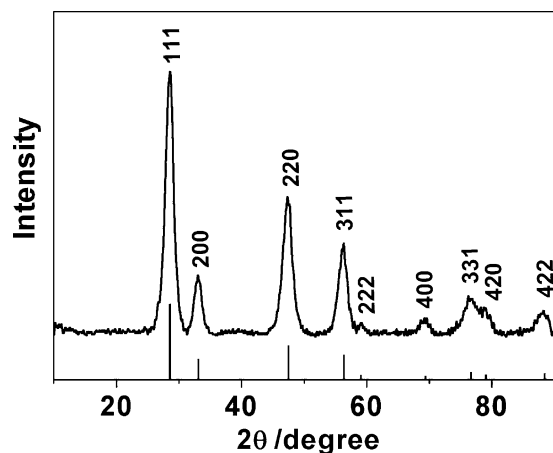


**Figure 2.** XRD pattern of CeO<sub>2</sub> nanorods.

orientations. The similar structure was observed in the previous reported CeO<sub>2</sub> nanowires.<sup>28</sup> The fast Fourier transform electron diffraction (ED) pattern in Figure 1c (inset) made from the single nanorod further confirms that the CeO<sub>2</sub> nanorods have a polycrystalline structure. The EDS spectrum in Figure 1d shows no detectable amount of Na, and only Ce (24.3%) and O (51.3%) are detected, suggesting that the nanorods are composed of CeO<sub>2</sub>, while the C and Cu peaks come from the Cu grids.

The phases of the obtained nanorods were examined by XRD. The diffraction peaks in Figure 2 correspond to the (111), (200), (220), (311), (222), (400), (311), (420), and (422) planes, which can be indexed to the face-centered cubic

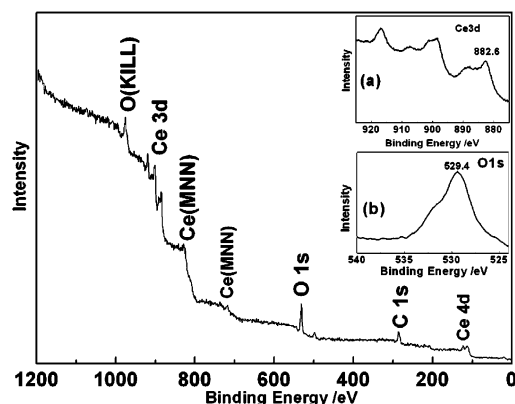


**Figure 3.** XPS wide spectrum of CeO<sub>2</sub> nanorods. Ce 3d (inset, a) and O 1s (inset, b) core level spectra of CeO<sub>2</sub> nanorods.

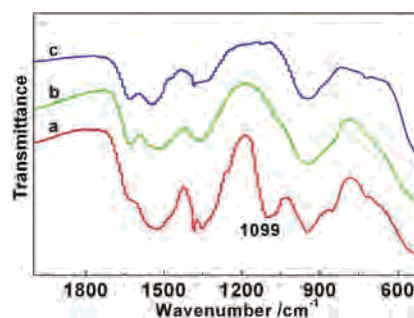


**Figure 4.** FT-IR spectra of water-washed (a) and alcohol-washed (b) CeO<sub>2</sub> nanorods and commercial CeO<sub>2</sub> powders (c).

structure for CeO<sub>2</sub> (space group *Fm3m*) with a lattice constant of  $a = 0.5410$  nm according to JCPDS 78-0694. The obtained CeO<sub>2</sub> nanorods are pure phase products. No obvious peaks corresponding to cerium nitrate or other cerium oxides were observed in the powder pattern.

Figure 3 depicts the XPS spectrum of the CeO<sub>2</sub> nanorods. Peaks of Ce 3d, O 1s, C 1s, and Ce 4d can be identified. No peaks ascribable to Na 2p are observed, indicating that the NaOH impurity was of trace amount.<sup>35</sup> According to the Ce 3d core level peak shown in Figure 3 (inset, a), it is obvious that the cerium exists in the Ce(IV) oxidation state (882.6 eV), without any impurity of the Ce(III) oxidation state.<sup>25</sup> In addition, the O 1s core level peak shown in Figure 3 (inset, b) centered at 529.4 eV corresponds to the O<sup>2-</sup> contribution.<sup>25,36</sup> Thus, the XPS-detected binding energies of Ce 3d and O 1s of the as-synthesized nanorods are in agreement with those of the standard CeO<sub>2</sub>.<sup>25,34</sup>

Figure 4 shows the FT-IR spectra of water-washed and alcohol-washed CeO<sub>2</sub> nanorods and commercial CeO<sub>2</sub> powders. In curve a, the peak at 1099 cm<sup>-1</sup> is assigned to the  $\nu_{as}$  (C–O–C) stretching vibrations from PEG. When compared with the corresponding peaks in curve b, the peak at 1099 cm<sup>-1</sup> disappears entirely after washing. Obviously the PEG is weakly adsorbed onto the surfaces of CeO<sub>2</sub> nanorods and has been removed entirely from the nanorods after alcohol washing. The FT-IR peaks of the alcohol-washed CeO<sub>2</sub> nanorods (Figure 4b) are similar to those of commercial CeO<sub>2</sub> powders (Figure 4c). The similar alcohol-washing manipula-

(36) Salvi, A. M.; Decker, F.; Varsano, F.; Speranza, G. *Surf. Interface Anal.* **2001**, *31*, 255.

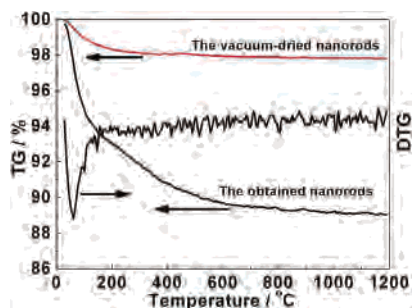


Figure 5. TG–DTG curves of CeO<sub>2</sub> nanorods.

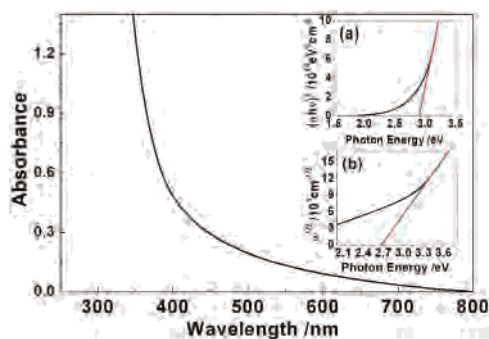


Figure 6. UV–vis spectrum of nanorods dispersed in ethanol. Plots of  $(\alpha h\nu)^2$  vs photon energy for nanorods (inset, a), and plots of  $\alpha^{1/2}$  vs photon energy for nanorods (inset, b).

tion was also conducted to Fe<sub>3</sub>O<sub>4</sub> nanorods,<sup>16</sup> ZnO nanorods,<sup>17</sup> and CuO nanorods.<sup>8</sup>

Figure 5 shows the TG analysis of the obtained nanorods. The mass loss is about 10.9 wt % below 1200 °C with only one peak around 100 °C in the DTG curve for the obtained nanorods. As we all know that CeO<sub>2</sub> can easily adsorb water molecules from the air due to hydrogen-bond formation on its surface,<sup>37</sup> it is obvious that the unique peak around 100 °C for the obtained nanorods is due to the loss of adsorbed water. The relatively higher content of adsorbed water can be explained as follows. The drying apparatus in our experiment is a closed system; the sample may easily adsorb water molecules with the higher steam vapor at higher temperature. To demonstrate our conclusion, the sample was vacuum-dried at 100 °C, and the TG curve shows that the mass loss is only about 2.1 wt %.

The UV–vis absorption spectrum of the CeO<sub>2</sub> nanorods is shown in Figure 6. The spectrum distinctly exhibits a strong absorption band at the UV region due to the charge-transfer transitions from O 2p to Ce 4f bonds, which overrun the well-known f to f spin–orbit splitting of the Ce 4f state.<sup>38</sup> According to previous analysis,<sup>23,39</sup> the plots of  $(\alpha h\nu)^2$  versus photon energy in Figure 6 (inset, a) show the direct band gap energy ( $E_d$ ) of 2.90 eV for CeO<sub>2</sub> nanorods, and the plots of  $\alpha^{1/2}$  versus photon energy in Figure 6 (inset, b) give the indirect band gap energy ( $E_i$ ) of 2.67 eV for CeO<sub>2</sub> nanorods. Previous reported data shows that  $E_d$  and  $E_i$  decrease with the increasing size of CeO<sub>2</sub> nanoparticles due to the quantum confinement effect.<sup>23,40</sup> Our values basically agree with those

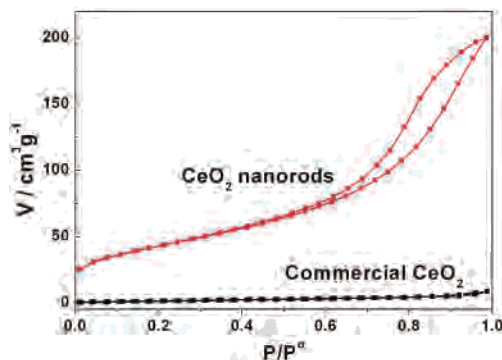


Figure 7. Nitrogen adsorption/desorption curves of CeO<sub>2</sub> nanorods and commercial CeO<sub>2</sub> powders.

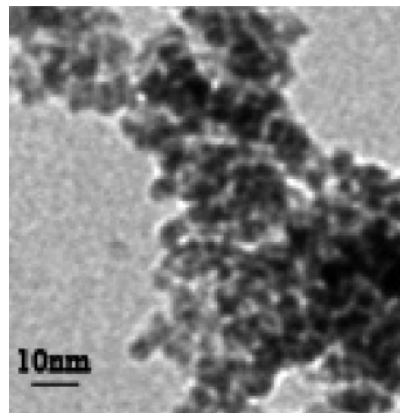


Figure 8. TEM image of the agglomerated CeO<sub>2</sub> nanoparticles prepared in the absence of PEG.

for CeO<sub>2</sub> nanoparticles synthesized by a microemulsion method ( $E_d$  is 3.44 eV for 2.6 nm and 3.38 eV for 4.1 nm, while  $E_i$  is 2.87 eV for 2.6 nm and 2.73 eV for 4.1 nm).<sup>40</sup>

As can be seen from Figure 7, CeO<sub>2</sub> nanorods present a type IV nitrogen adsorption isotherm, with a hysteresis loop where the desorption required definitively higher energy than adsorption.<sup>41</sup> The hysteresis of CeO<sub>2</sub> nanorods is definitively more pronounced than that of commercial CeO<sub>2</sub>. It is calculated that the BET specific surface area of CeO<sub>2</sub> nanorods is 154.5 m<sup>2</sup> g<sup>-1</sup>, while that of commercial CeO<sub>2</sub> is 5.7 m<sup>2</sup> g<sup>-1</sup>. In our case, the BET specific surface area of CeO<sub>2</sub> nanorods is much higher than that of the nanorods synthesized by a hydrothermal method (~50 m<sup>2</sup> g<sup>-1</sup>).<sup>24</sup>

#### Factors Affecting the Formation of CeO<sub>2</sub> Nanorods.

In this preparation experiment, the surfactant PEG plays an important role in the formation of CeO<sub>2</sub> nanorods. When the reaction was carried out without the aid of PEG, no nanorods but the agglomerated nanoparticles as the sole product were observed in Figure 8. This can be explained as follows. Under basic conditions, OH<sup>-</sup> ions were predominantly adsorbed onto the surface of CeO<sub>2</sub>, giving rise to the existence of a large portion of surface hydroxyls for the obtained CeO<sub>2</sub> nanocrystals.<sup>42</sup> The aggregation was caused

(37) Djuricic, B.; Pickering, S. *J. Eur. Ceram. Soc.* **1999**, *19*, 1925.

(38) Tsunekawa, S.; Fukuda, T. *J. Appl. Phys.* **1999**, *87*, 1318.

(39) Leeuwen, R. A. V.; Hung, C.-J.; Kammler, D. R.; Switzer, J. A. *J. Phys. Chem.* **1995**, *99*, 15247.

(40) Masui, T.; Fujiwara, K.; Machida, K.; Adachi, G. *Chem. Mater.* **1997**, *9*, 2197.

(41) Frackowiak, E.; Delpeux, S.; Jurewicz, K.; Szostak, K.; Cazorla-Amoros, D.; Béguin, F. *Chem. Phys. Lett.* **2002**, *361*, 35.

(42) Si, R.; Zhang, Y.-W.; You, L.-P.; Yan, C.-H. *J. Phys. Chem. B* **2006**, *110*, 5994.

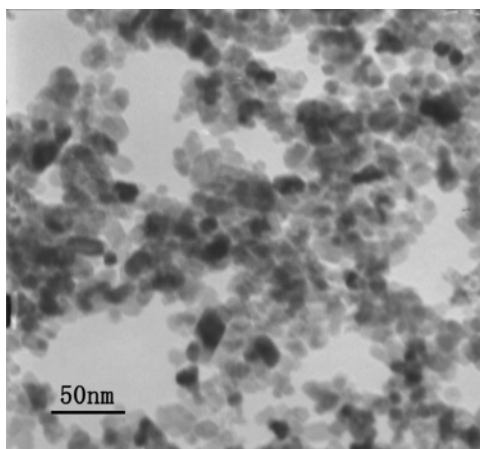
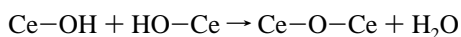


**Figure 9.** TEM image of the as-synthesized sample without ultrasonic radiation.

by the attraction from the elimination of surface hydroxyls on the adjacent particles via a condensation reaction dehydration between two surfaces under basic conditions,<sup>42,43</sup> as follows:



It is noted that the colloidal  $\text{CeO}_2$  solution can easily precipitate, while the PEG-added colloidal solution can stably exist, indicating that PEG was adsorbed onto the surfaces of the colloidal  $\text{CeO}_2$  nanoparticles. However, the steric hindrance effect of PEG was relatively weaker than the oriented aggregation caused by the condensations between surface hydroxyls, especially in the ultrasonic radiation. According to the oriented attachment mechanism suggested by Banfield and co-workers, the adjacent nanoparticles spontaneously self-organized so that they share a common crystallographic orientation, followed by the joining of these particles at a planar interface.<sup>44,45</sup> During the oriented attachment, bonding between the nanoparticles reduces the total energy by removing surface energy associated with unsatisfied bonds.<sup>44,45</sup> In our case,  $\text{CeO}_2$  nanocrystals fused to each other by facets and grew as a whole, and then the  $\text{CeO}_2$  nanorods formed, which is the same as the formation of Au and Ag nanowires reported by Maddanimath et al.<sup>46</sup>

To investigate the role of ultrasonication in the formation of the nanorods, the control reactions employed by vigorous agitation without ultrasound at various temperatures (25, 40, and 60 °C) were conducted with other conditions unchanged. No nanorods but nanoparticles as the sole products were observed, even with a longer reaction time. The typical TEM image of the nanoparticles is shown in Figure 9. The resultant nanoparticles are ~20 nm in size. It can be found that ultrasonication is a key factor to the formation of nanorods. The action principle of ultrasonication is discussed in following text (the possible formation mechanism of  $\text{CeO}_2$  nanorods).

(43) Nabavi, M.; Spalla, O.; Cabane, B. *J. Colloid Interface Sci.* **1993**, *160*, 459.

(44) Penn, R. L.; Banfield, J. F. *Science* **1998**, *281*, 969.

(45) Banfield, J. F.; Welch, S. A.; Zhang, H.-Z.; Ebert, T. T.; Penn, R. L. *Science* **2000**, *289*, 751.

(46) Maddanimath, T.; Kumar, A.; D'Arcy-Gall, J.; Ganesan, P. G.; Vijayamohan, K.; Ramanath, G. *Chem. Commun.* **2005**, 1435.

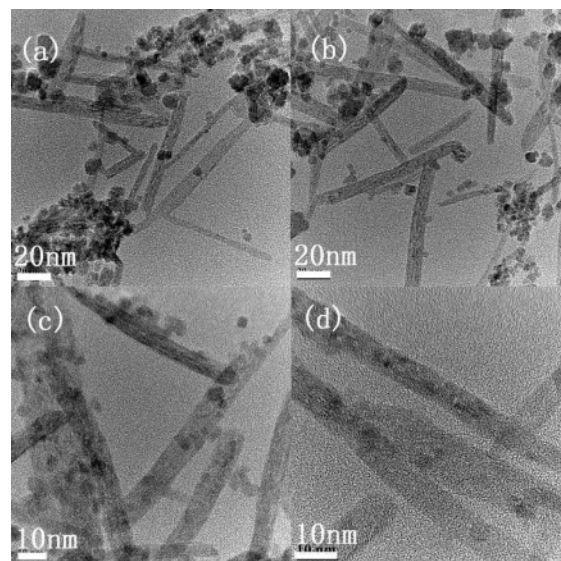


**Figure 10.** TEM images of  $\text{CeO}_2$ . (a) The sample without subsequent sonication; (b) the sample sonicated for 10 min; (c) the sample sonicated for 30 min; (d) the sample sonicated for 1 h.

A series of control experiments were carried out to investigate the effects of the content of PEG, the molecular weight of PEG, the concentration of KOH, and the pH value. It is found that the concentration of KOH (0.001–0.1 g/mL) and the pH value (7–12) have a slight effect on the morphologies of  $\text{CeO}_2$ . The resultant products without subsequent sonication include both nanorods and nanoparticles, and the ratio between nanorods and nanoparticles varies slightly. However, the content of PEG plays an important role in the formation of nanorods. The main products are nanorods with a small quantity of nanoparticles in a range of PEG content (0.5%–5%), while the main products are agglomerated nanoparticles and dispersed nanoparticles at a lower content (<0.5%) and a higher content (>5%) of PEG, respectively. It can be explained that too low a content of PEG cannot confine much area of the colloids while too high a content of PEG confined all aspects of the colloids.<sup>17</sup> Similar phenomena are also observed in the CTMABr-assisted formation of  $\text{CeO}_2$  nanorods by a hydrothermal method.<sup>29</sup>

PEG200, PEG600, PEG2000, and PEG20000 are employed to investigate the role of the molecular weight of PEG. It is found that the ratio between nanorods and nanoparticles varies slightly by using PEG200, PEG600, and PEG2000, while the presence of nanorods is distinctly reduced by using PEG20000. It can be explained that PEG with high molecular weight has a strong steric hindrance, which confines the fusing of nanoparticles.<sup>17</sup> The phenomena are also found in the formation of ZnO nanowires with various molecular weights of PEG by a hydrothermal method.<sup>17</sup>

According to experimental data, we found that the exclusive nanorods are hard to obtain directly without the subsequent sonication. The subsequent sonication time is effective in promoting the formation of nanorods. We carried out a series of experiment in which the colloidal precipitates were sonicated for various times. Figure 10 shows that with the subsequent sonication time increasing, more and more

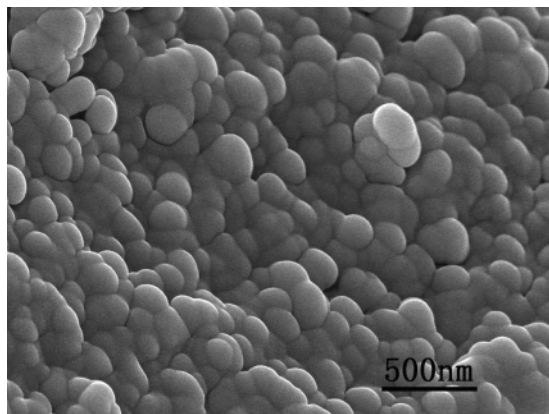
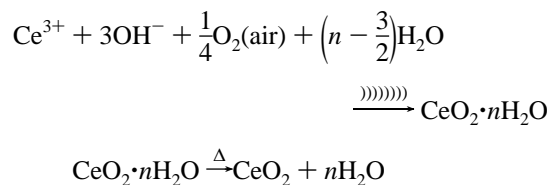


**Figure 11.** SEM image of the as-synthesized product aged for days without ultrasonication.

nanoparticles disappear, and finally the nanorods are nearly the sole product, indicating that the nanorods grow from the tiny nanoparticles. From the HRTEM image of the single nanorod shown in Figure 1c, it is clear that the nanorods are indeed built from nanoparticles. Similar phenomena are also found in the formation of metal nanowires from nanoparticles by Maddanimath et al.<sup>46</sup> It is noted that the colloidal solution was prepared first without ultrasonication and then sonicated for various times, and similar phenomena are observed. However, to obtain the sole nanorods in this process, it takes ~2 h, which is equivalent to the total sonication time of the above-mentioned experiment.

The colloidal precipitates (the mixture of nanorods and nanoparticles) aged for days without the subsequent sonication were also investigated. The resultant products are shown in Figure 11. It is interesting that the nanorods disappear entirely and the spherical particles with diameter of ~100 nm are formed. This process can be explained by an Ostwald ripening growth mechanism where the larger particles grow at the expense of the smaller particles.<sup>47</sup> In addition, due to the weak excluding force of PEG, the nanoparticles fused together from various orientations, and thus the spherical particles with the larger size are obtained.

**Possible Formation Mechanism of CeO<sub>2</sub> Nanorods.** It is well-known that the Ce(III) oxidation state is unstable as compared with the Ce(IV) oxidation state in alkaline solution and in the presence of air. According to the above analysis, sonication of an aqueous solution of cerium(III) nitrate with addition of the alkaline solution results in the formation of hydrated cerium(IV) oxide:



**Scheme 1.** Possible Formation Mechanism of CeO<sub>2</sub> Nanorods



The formation of the nanorods may be explained as follows. The CeO<sub>2</sub> nanoparticles adsorb OH<sup>-</sup> ions on their surfaces, thus fusing them by hydrogen bonding, but PEG could favor relatively strongly oriented aggregations. It is well-known that the strongly adsorbed stabilizer prevents the aggregation between colloidal nanoparticles due to its steric hindrance effect.<sup>48</sup> In our experiment, PEG was weakly adsorbed onto the surfaces of CeO<sub>2</sub> nanocrystals and could play the bridge-linking role since PEG has a linear structure and multiple coordinating sites. In addition, with the aid of ultrasonication, the generated bubbles collapse asymmetrically, resulting in the generation of high-speed microjets,<sup>49</sup> the velocity of which may be very high. Due to this very high velocity of the liquid jets, the chance of collision between two PEG-adsorbed nanoparticles increased. As a result, more nanocrystals fused in an oriented manner, and then CeO<sub>2</sub> nanorods formed. The special effect of the ultrasonication in preparation of the 1-D nanostructure has been demonstrated by Pol et al.<sup>14</sup> According to these deductions, the formation mechanism of CeO<sub>2</sub> nanorods was proposed as depicted in Scheme 1.

## Conclusion

In summary, polycrystalline CeO<sub>2</sub> nanorods 5–10 nm in diameter and 50–150 nm in length have been successfully prepared using PEG as a structure-directing agent by an ultrasonic method. The content of PEG, the molecular weight of PEG, and the sonication time were confirmed to be the crucial factors determining the formation of 1-D CeO<sub>2</sub> nanorods. Such nanorods with higher surface area are very interesting for further studies on their physical and chemical properties. The versatility of this method could be extended to other metal oxide nanorods.

**Acknowledgment.** This work was supported by Nano-Science & Technology Special Project (0452nm027) of Shanghai, China.

IC061697D

- (47) Talapin, D. V.; Rogach, A. L.; Shevchenko, E. V.; Kornowski, A.; Haase, M.; Weller, H. *J. Am. Chem. Soc.* **2002**, *124*, 5782.  
 (48) Spalla, O.; Nabavi, M.; Minter, J.; Cabane, B. *Colloid Polym. Sci.* **1996**, *274*, 555.  
 (49) Doktycz, S. J.; Suslick, K. S. *Science* **1990**, *247*, 1067.